J. Jpn. Soc. Microgravity Appl. Vol. 28 No. 2 2011 (S17–S22)

8th Japan-China-Korea Workshop on Microgravity Sciences
for Asian Microgravity Pre-Symposium

Colloidal Gas-Liquid-Solid Phase Diagram in Low Ionic Strength Solutions

Masamichi ISHIKAWA [1] and Ryota KITANO [2]

Abstract

Polystyrene latex particles showed gas-liquid condensation under the conditions of large particle radius ($a >> \kappa^{-1}$) and intermediate κa, where κ is the Debye-Hückel parameter and a is the particle radius. The particles were dissolved in deionized water containing ethanol from 0 to 77 vol.% settled to the bottom of the glass plate within 1 hour and, then, laterally moved toward the center of a cell over a 20 hour period in reaching a state of equilibrium condensation. All the suspensions of 1 and 3 μm in diameter and of 0.01-0.20 vol.% in concentration realized similar gas-liquid condensation with clear gas-liquid boundaries. A phase diagram of the gas-liquid condensation was created as a function of KCl concentration at a particle diameter of 3 μm, 0.10 vol.% in concentration, and 50:50 water/ethanol solvent at room temperature. The miscibility gap was observed in the concentration range from 1 to 250 μM. There was an upper limit of salt concentration where the phase separation disappeared, showing near critical behavior of macroscopic density fluctuation from 250 μM to 1 mM. These results add new experimental evidence to the existence of colloidal gas-liquid condensation and specify conditions of like-charge attraction between particles.

1. Introduction

Gas-liquid phase separation analogous to vapor-liquid condensation in atomic systems has been studied in dilute and deionized colloidal suspensions of polystyrene particles[1)]. After theoretician's acceptance of the void formation in the density matched colloidal suspension, the role of like-charge attraction between colloidal particles in causing colloidal phase separation was debated [2)]. However, it is often claimed that the range of the miscibility gap in the gas-liquid condensation experiments has not been clearly identified in any kind of phase diagram, such that it presents the range of the instability.

Van Roij et al., Levin et al. and Warren proposed a van der Waals-like instability of charge-stabilized colloidal suspensions based on linear Poisson-Boltzmann theory [3-9)]. The essence of their argument is the full evaluation of free energy terms which relate the interactions between macroion-small ion, macroion-macroion, and small ion-small ion. Tamashiro and Schiessel raised objections to the validity of their linear theory, in particular, to whether or not the gas-liquid phase instabilities are mathematical artifacts of the linearization approximation, because the evaluation of nonlinear Poisson-Boltzmann theory showed no miscibility gap[10)]. Addressing that point, Zoetekouw and van Roij again reported the positive correspondence of the nonlinear version of their theoretical instability with experimental results, introducing the criteria of $Zl_B/a \geq 24$, where Z is the charge, a is the radius, and l_B is the Bjerrum length[11)]. These discussions assumed the weak coupling limit of low volume fraction of colloids, low surface charge density, low counterion valency, and high temperature. Netz further analyzed the opposite limit of strong coupling and showed the existence of the attraction of like-charged macroions by considering the counterion condensation process that directly affects the effective interactions[12, 13)].

The counterion condensation has been known in polyelectrolyte solutions. Manning proposed a model of simple polyelectrolytes[14-16)]. This condensation results in an effective charge saturation due to the screening of the surface charge by counterions and coions, which are treated theoretically as the charge renormalization in the Debye-Hückel theory[17-18)]. The effective charge changes drastically according to the bare charge of the particle because with increasing bare charge, the ionic density in the electrical double layer grows nonlinearly too large. In the field of electrophoresis measurement, it is well known that counterion condensation around charged colloids has an important effect on zeta potential measurements. Fluid flow of the surrounding solution and the external electrical field deform the double layer when its thickness is approximately located at the surface of shear. This phenomenon, called the relaxation effect, has been extensively studied to relate the electrophoretic mobility with the ζ potential around a particle[19-21)]. The effect is prominent in the range of intermediate κa with values ranging from 5 to 150. Latex particles with a diameter exceeding 1 μm show the relaxation effect in the relatively low ionic strength solution. Colloidal gas-liquid phase separation is proposed to be a consequence of the nonlinear many-body interaction between the particles with the surrounding ionic atmosphere as described in detail by Warren[9)]. When $a >> \kappa^{-1}$ (κ = Debye-

1 RIKEN, 2-1 Hirosawa, Wako, Saitama, 351-0198, Japan.
2 AGC Electronics Co. Ltd., 1-2 Machi-ikedai, Koriyama, Fukushima 963-0215, Japan.
(E-mail: masamichi.ishikawa @riken.jp)

Hückel parameter), the nonlinear effects are confined to be in the immediate vicinity of macroions with an extension of κ^{-1}. Therefore, the charged colloids with a large diameter and intermediate κa may behave according to the linear Poisson-Boltzmann theory. This kind of experimental condition has the potential to examine the phase instability, because nonlinear interactions activate the attraction between particles, while the linear approximation is still valid in the analytical treatment. Unfortunately, there are few gas–liquid condensation experiments using large particles with such intermediate κa.

We have found an equilibrated phase separation of the colloidal suspension in the condition of intermediate κa. Although the particles used were relatively large, they still migrated upward against the gravitational force due to Brownian agitation. To confine their presence in a mono-particle layer for further quantitative treatment, we enforced the sedimentation of the particles by adjusting the solvent density. This caused mono-particle layer condensation at the bottom of the experimental cell, but still floated above the bottom glass surface due to electrostatic repulsion. As a result, all the particles initially sedimented to the bottom and, then, laterally condensed toward the center of the cell. An important parameter to consider is the effective surface charges of the macroions in the analytical evaluation of the phase instabilities under the imposed experimental conditions. We determined the effective surface charges using an electrophoretic mobility measurement, and their validity was checked by comparison with the relationships derived from the linear Poisson-Boltzmann theory.

2. Experimental

The colloidal particles of sulfonated polystyrene (PS) microsphere (diameter, 1 and 3 μm) were obtained from Duke Sci. Corp., and treated by a mixed-bed ion exchange resin, Bio-RAD-501-X8(D) for approximately one month. The experimental cell was made of crown glass with a disk-shaped inner volume with a 10.0 mm diameter and 0.5 mm thickness as shown in **Fig. 1**. The glass surface was processed with the flatness of 4 nm. The lower and middle glass plates were bonded by a plastic agent. The upper glass was sealed using vacuum grease and air bubbles were carefully excluded when each sample was filled. The cell was located on a flat and horizontal metal plate to diminish a temperature gradient and an inclination to gravity. The particle concentration was varied from 0.001 to 0.23 vol.%. Sedimentation force was enhanced to realize the mono–particle layer condensation on the bottom plate of the cell by mixing water with ethanol at a volume ratio from 0 to 77%. Both solvents were fully deionized by the ion exchange resin in advance. The density of the solvent was determined such that nearly 100% of the particles were distributed within the thickness of their diameter, assuming the sedimentation equilibrium density profile $n(z)$ [22, 23].

$$n(z) = n_0 \exp\left(-\frac{zPe}{h}\right) \qquad (1)$$

where z is the height from the bottom of the cell, n_0 is the particle number at $z = 0$, h is the height of the cell, $Pe = hU_0/D$, Pe is the Peclet number, U_0 is the stationary-state sedimentation velocity, and D is the diffusion coefficient. The mono-particle layer sedimentation was confirmed using confocal laser scanning microscopy (CLSM). Optical microscopy was used for in-situ observation of the colloidal condensation at the bottom of the cell. KCl was added as a salt with concentration ranging from 1~1000 μM. All the experiments were performed at room temperature.

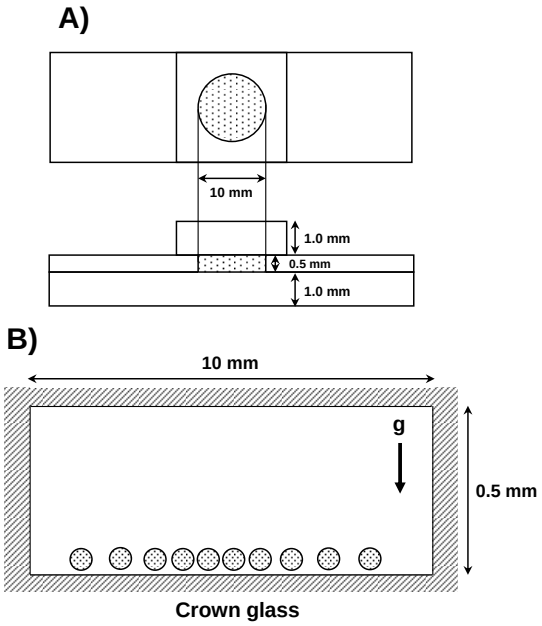

Fig. 1 Experimental set up of colloidal phase separation. The optical cell, made of crown glass, with 10 mm diameter and 0.5 mm thickness (A). The Gravitational sedimentation of polystyrene latex was enhanced by adjusting the solvent density by mixing 50:50 water/ethanol, and the mono-particle layer was maintained during the liquid phase condensation (B).

The measurements of the zeta potential of colloids in various salt solutions were accomplished by a electrophoretic mobility measurement. The particle mobility under an applied electric field was determined by tracing their loci in real time using a ZEECOM zeta potential analyzer (Microtec Co. Ltd. Japan). Using the average mobility data of 100 particles, zeta potentials of the particles in each salt concentration were evaluated using the analytical equation 4.20 in the paper of O'Brien and Hunter[19]. When the measured sample was in the range of intermediate κa, this equation has a maximum mobility

above 40 mV in the absolute value of the zeta potential, so that two zeta potentials (low and high values) were found. The surface charge densities of colloids and glass were calculated according to the linear Poisson-Boltzmann theory as described elsewhere [24].

3. Results and Discussion

Gas-liquid condensation was observed for both 1 μm and 3 μm suspensions in a wide range of concentrations, 0.001-0.20 vol.% and 0.01-0.23 vol.%, respectively. Homogeneous samples with varying particle, EtOH, and salt concentrations equally sedimented to the bottom plate of the cell within 1 hour and gradually condensed over 20 hours. In the aqueous solvent containing more than 50 vol.% EtOH, it was confirmed using CLSM that 3 μm suspensions settled to the bottom plate in a mono-particle layer thickness. On the other hand, 1 μm suspensions formed thick condensed layers at the bottom. Interestingly, 3 μm suspensions under the conditions of more than 0.10 vol.% and 50 vol.% EtOH showed a coexistence of the gas, liquid and solid (ordered) phases located from the peripheral of the condensates to the center.

We observed the phase separation in detail using 3 μm suspensions at 0.10 vol.%, 50% EtOH, with no added salt. **Figure 2-A** shows an example of such gas-liquid phase separation. Since sedimentation was enhanced by reducing the solvent density, the time scale of the sedimentation became much shorter than that of the condensation, and as a result a separate observation was possible. The quantitative measurements of the particle-existing area (white area) were made by the image processing method. This area decreased with time and reached a constant value (77% of the bottom plate) as shown in **Fig. 2-B**. A magnified boundary between the liquid phase and the gas phase is also indicated in **Fig. 2-C**. The particle arrangements showed sparseness at the edge of the boundary and more dense condensation inside the boundary, indicating the attractive interaction of the periphery particles with the inside particles.

In order to determine the region of observed miscibility gap, a phase diagram was investigated in the volume fraction-salt concentration expression. The phase diagram was constructed at a constant particle number (2.77×10^6, 0.10 vol.%) at room temperature. Figure 3 shows the phase diagram in water/EtOH (50:50) with respect to volume fraction and added salt concentration. The volume fraction was calculated according to the relationship, $\phi = (4/3)\pi a^3 N_0 / 2aS$, where N_0 is the number of the added particles and S is the area of the bottom plate. The dotted line in **Fig. 3** is the initial volume fraction calculated assuming that the total particles settled to a mono particle layer on the bottom plate. The low and high error bars were drawn using the densities at the peripheral and the center of a condensate, respectively. Thus, the difference between the dotted line and the volume fraction of the condensed phase shows a miscibility gap, extending from 1 to 1000 μM salt concentration as shown in **Fig. 3**.

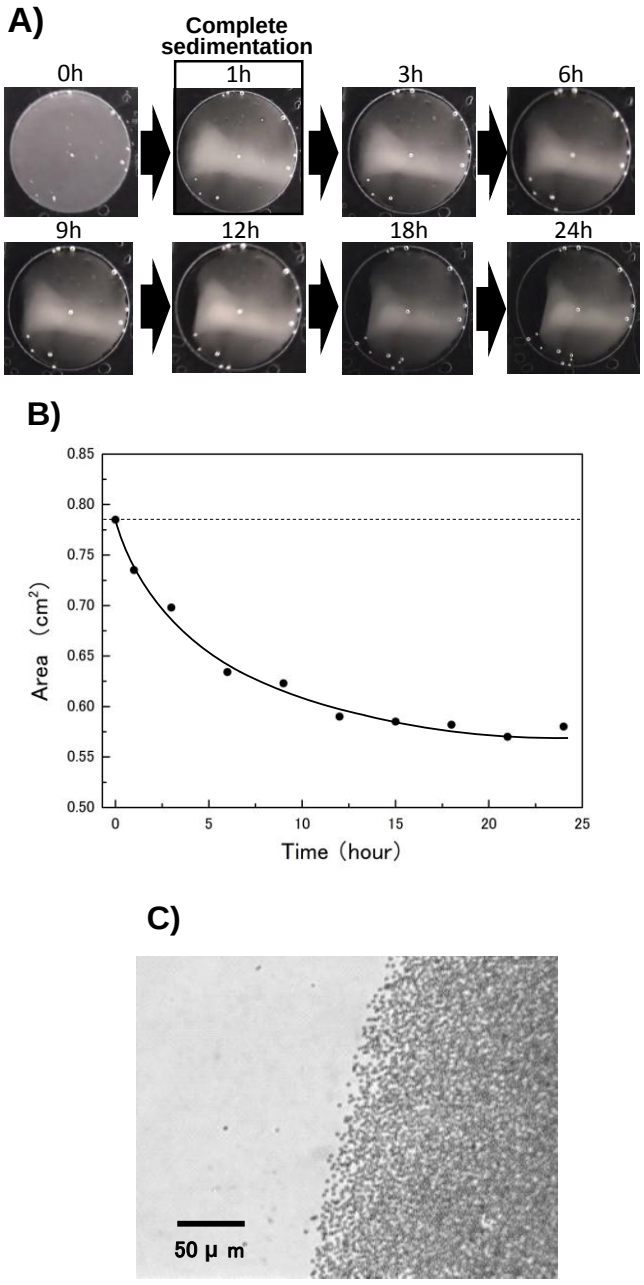

Fig. 2 A series of photographs of liquid phase condensation (white part) after the homogeneous dispersion of colloidal particle (diameter 3 μm) at 0.10 vol.%, as a function of time (A). The white small circles in the photographs are air bubbles. The change of the particle condensation area (white part) was determined by the image processing method (B). The dotted line shows the bottom plate area. The magnified gas-liquid phase boundary after 25 hours (C).

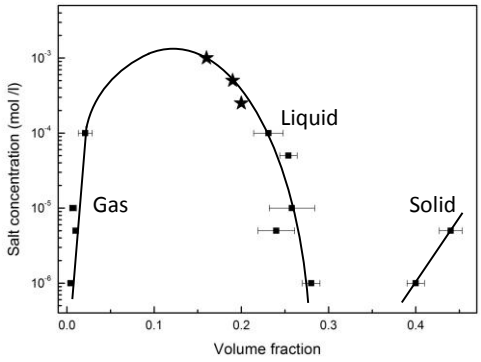

Fig. 3 A colloidal gas-liquid-solid phase diagram in the volume fraction-salt concentration expression. Polystyrene particles were sedimented in the mono-particle layer at the bottom of the observation cell, at the initial homogeneous particle concentration 0.10 vol.%. The star symbol indicates the appearance of the near critical phase separation showing the large scale wave like density fluctuation as shown in **Fig. 4-A**.

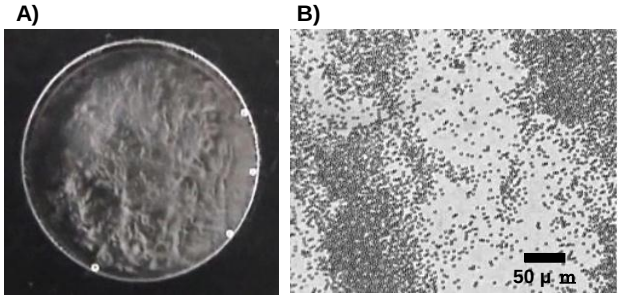

Fig. 4 Photograph of abnormal density fluctuation (white part) observed at a salt concentration of 500 μM KCl (A), and magnified photograph of density fluctuation showing a striated structure (B).

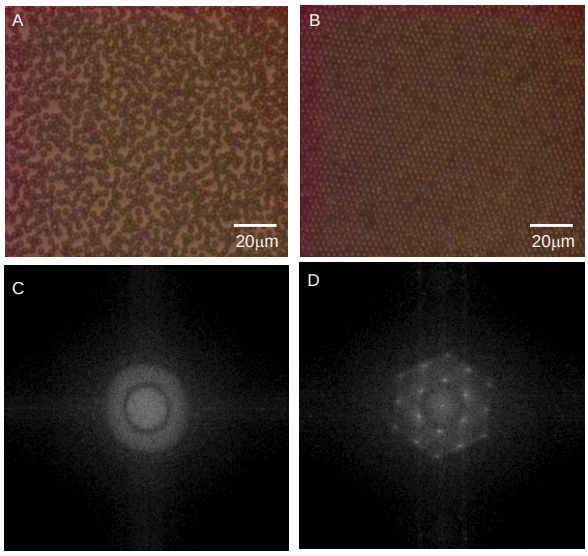

Fig. 5 Coexistence of the liquid and solid phases. Liquid region (A), ordered region (B), and Fourier transform patterns of the liquid and solid phases (C) and (D), respectively.

An interesting feature of the instability is the appearance of a near-critical density fluctuation in the vicinity of the upper bound of the miscibility gap (250-500 μM, KCl). **Figure 4-A** indicates a wave-like inhomogeneity extended over the whole area of the cell. **Figure 4-B** also shows a magnified view of the inhomogeniety, where dense and depleted areas were striated nearly 100 μm in width. Nabutovskii et al. reported the appearance of a charge density wave (CDW) phase near the critical point[25]. The wave-like inhomogeneity is thought to appear due to a long-range colloidal density fluctuation in the vicinity of the critical point to form the macroscopic dipolar structure of colloidal with rich and depleted phases, where electrical double layer formed around the rich phase by a charge neutralization requirement. Here, we only mention the appearance of the abnormal density fluctuation in the experiment and its relevance to Warren's theoretical prospect[9], leaving its detailed analysis for future study.

Figure 5 shows another interesting aspect of the gas-liquid phase separation. When the liquid phase condensation proceeded under enhanced sedimentation, the increase of particle concentration at the center of the cell caused an order-disorder transition as shown in **Fig. 5-A and B**. **Figure 5-C and D** show Fourier transform patterns of images A and B, respectively. The observation clearly shows a mechanism of colloidal crystallization where the attractive force between the particles realized a packing density which triggered the Kirkwood-Alder transition.

The experimental results showed an attractive nature of particle interactions. Next, we evaluated the origin of the miscibility gap according to the linear Poisson-Boltzmann theory. We assume that the validity of linear theory is based on a large particle radius ($a >> \kappa^{-1}$) [15] and weak coupling with salt ions[12]. In order to evaluate the appearance of the miscibility gap according to linear theory, the effective charges on the particles are necessary for the accurate estimation of the free energy term of the interactions. We measured the effective charges by the electrophoresis method. Zeta potentials were calculated from the electrophoretic mobility data using the equation derived by O'Brien and Hunter[19]. Since small ions accumulate around highly charged particles, it is not the bare charge that determines the mobility, but rather the effective (or renormalized) charge. In order to derive a formula for the mobility of a large particle, it is necessary to take the distortion of the double layer into account. As pointed out by O'Brien and White, there is a maximum of the electrophoretic mobility as a function of the zeta potential in the intermediate κa value (5 to 150), that is, the low and high values of the zeta potential are assigned when the mobility is obtained. The ionic environment surrounding a macroion deforms by both particle movement and external electric field. The appearance of the mobility maximum is formulated by

introducing the relaxation term of the fluid mechanical deformation of the electrical double layer whose periphery coincides with the shear plane due to decreasing Debye length. The fluidity of the electrical double layer shall indicate a many-body interaction between macroions via redistributing surrounding counter-ions.

Table 1 shows the results of zeta potential measurements at both low and high values for each salt concentration. The absolute values increased with increasing salt concentration. According to the numerical solution of the Poisson-Boltzmann equation of spherical colloids, the effective surface charge increases with increasing structural charge of macroions before finally saturating at what is called the effective charge saturation [17, 18]. Since the saturated effective charge increases with κ, we can test the charge saturation in our experimental conditions using the obtained data as reported elsewhere [24].

In order to evaluate the instability conditions, osmotic compressibility under the experimental parameters of observed phase instabilities was calculated following the method of the free energy calculations for highly asymmetric electrolytes[9]. We suppose that the colloidal particles or macroions with a diameter $\sigma = 2a$, negative charge $|Z|>>1$ and number density n_m There are small coions and counter ions at number density n_- and n_+, respectively. The solvent is taken to be a dielectric continuum of permittivity $\varepsilon=\varepsilon_0\varepsilon_r$, where ε_0 and ε_r are the permittivity of vacuum and relative permittivity of the solvent, respectively. The coulomb interaction between a pair of univalent charges in units of kT is l_B. The densities are related by the electroneutrality condition $Zn_m + n_- = n_+$, and $n_- = n_s$, where n_s is the number density of salt ions. The Debye screening length is defined as

$$\kappa^2 = 4\pi l_B(n_+ + n_-) = 4\pi l_B(Zn_m + n_s) \qquad (2)$$

The free energy of colloidal phase separation is analytically defined by summing five elementary energy terms: ideal gas, macroion-small ion interaction, macroion-macroion interaction, hard core interaction, and small ion-small ion interaction, in order of relative importance. If we restrict our analysis to gas-liquid phase separation, two free energy terms are enough to estimate the upper limit of the salt concentration, that is, the ideal gas term F_{id} of macroions and small ions, and the electrostatic term F_{ms} of macroions surrounded by small ions. The ideal gas term of macroions and small ions is:

$$\frac{F_{id}}{VkT} = n_m \log n_m + n_s \log n_s + (Zn_m + n_s)\log(Zn_m + n_s) \qquad (3)$$

The electrostatic term of macroions is obtained as Eq. (4), assuming the pair correlation method and the Debye-Hückel approximation [9]:

$$\frac{F_{ms}}{VkT} = -\frac{2}{3}Z^2 l_B \kappa n_m f(\kappa a) \qquad (4)$$

where

$$f(x) = \frac{3}{x^3}\left[\log(1+x) - x + \frac{x^2}{2}\right]$$

Osmotic compressibility (ρ) is defined as Eq. (5).

$$\rho = -\frac{1}{V}\left(\frac{\partial V}{\partial P}\right) = -n_m \frac{\partial(1/n_m)}{\partial P} \qquad (5)$$

If ρ is negative, the colloidal suspension is unstable, indicating that a miscibility gap is present. Then, osmotic pressure P is defined according to the following relations:

$$F \approx F_{id} + F_{ms} \qquad (6)$$

$$\beta P = \left(n_m\mu_m + n_s\mu_s - \frac{F}{V}\right)\beta \qquad (7)$$

and n_s, which is obtained by combining Eqs. (3), (4), (6), and (7). The maximum salt concentrations of immiscibility were calculated by evaluating the values changing the sign of ρ from negative to positive with increasing salt concentration. The used parameters were $Z = Z_{eff}$ (1.23×10^6 and 3.39×10^6, respectively), $n_m = 1.18 \times 10^{10}/\mathrm{cm}^3$, and l_B=1.09 nm (relative permittivity 51.43 of 50 vol.% ethanol/water at 25 °C was used; Handbook of Chemistry and Physics, CRC, 2003). The 1.31 mM (1.23×10^6) and 10.1 mM (3.39×10^6) were obtained as the maximum salt concentrations. The 1.31 mM was in good agreement with the upper limit of gas-liquid immiscibility as shown in **Fig. 3**, while the value 10.1 mM at the high charge was too large to compare with the experimental observation. We further obtained the critical salt concentration, by calculating spinodal curve as a function of n_m at the charge of 1.23×10^6. A maximum pressure of spinodal curve was obtained at $n_m = 0.950 \times 10^{10}/\mathrm{cm}^3$ and [KCl]=1.31 mM, indicating that the experimental particle concentration was in the vicinity of critical point and the observed abnormal density fluctuation near the critical concentration showed an aspect of CDW. The effective charge of 1.23×10^6 was 100 times larger than the highest value used in the theoretician's work. If we compare the calculated critical concentration 1.31 mM with, for example, 25 μM in the case of low surface charge particle (radius=326 nm and Z=7300) [5], the experimental immiscibility extended to the higher salt concentration is quite reasonable.

Table 1 Measurements of zeta (ζ)-potential and estimated effective surface charges assuming the electrical potential of the Debye-Hückel theory. N.D. indicates a divergence of the mobility function by O'Brien and Hunter[19]

KCl (M)	κa	Low value		High value	
		ζ (mV)	Z_{eff}	ζ (mV)	Z_{eff}
10^{-6}	4.9	-39.5	1.95×10^4	N.D.	N.D.
10^{-5}	15.6	-52.2	7.26×10^4	-235	3.27×10^5
10^{-4}	45	-76.8	2.96×10^5	-213	8.21×10^5
10^{-3}	156	-93.9	1.23×10^6	-258	3.39×10^6

4. Conclusion

We studied the anomalous gas-liquid condensation of colloidal suspensions and attributed its primary driving force to the electrostatic macroion-small ion interaction as proposed by van Roij, Warren and others. The appearance of the instability was confirmed by calculating the osmotic pressure of the colloidal suspensions as a function of salt and particle concentrations, where the effective charges of colloids obtained by the zeta potential measurement were used in the application of the Debye-Hückel theory. The calculation showed a miscibility gap below a maximum KCl concentration of 1.31 mM and explained the experimental limit of the colloidal phase separation. The effect of glass wall was examined by measuring the ratio of charge density between glass wall and colloidal particle. Although it is known that charged glass wall induces attractive effective potential between particles at low ionic strength, we estimated it as a secondary factor which assisted the phase separation.

The electrical double layer of highly charged particles of intermediate κa is characterized by highly screened and dense ionic atmosphere, so that the nonlinearity of the Poisson-Boltzmann equation of the charged interface is confined within the length of the Debye length (much smaller than the particle radius). This enables one to replace the effective charges by the renormalized surface charges. In this study, the charges experimentally obtained by the zeta potential measurement were confirmed to match well with the saturated surface charges of large particles. Such saturation indicates the strong charge renormalization by counterions, which may make it possible to explain gas-liquid condensation within the linear theory of the Poisson-Boltzmann equation.

Acknowledgement

They are grateful to Tsutomu Kajino for supporting the zeta potential measurement. This research was partially supported by the Ministry of Education, Science, Sports and Culture, Grant-in-Aid for 4901, 20200004, 2008.

References

1) B. V. R. Tata and S. S. Jena: Solid State Commun., **139** (2006) 562.
2) (a) K. Ito, H. Yoshida and N. Ise: Science, **263** (1994) 66. (b) H. Yoshida, N. Ise and T. Hashimoto: J. Chem. Phys., **103** (1995) 10146.
3) R. van Roij and J. P. Hansen: Phys. Rev. Lett., **79** (1997) 3082.
4) R. van Roij, M. Dijkstra and J. P. Hansen: J. P. Phys. Rev. E, **59** (1999) 2010.
5) B. Zoetekouw ad R. van Roij: Phys. Rev. E, **73** (2006) 021403.
6) Y. Levin, M. C. Barbosa and M. N. Tmashiro: Europhys. Lett., **41** (1998) 123.
7) M. N. Tmashiro, Y. Levin, M. C. Barbosa: Physica A, **258** (1998) 341.
8) A. Diehl, M. C. Barbosa and Y. Levin : Europhys. Lett., **53** (2001) 86.
9) P. B. Warren: J. Chem. Phys., **112** (2000) 4683.
10) M. N. Tmashiro and H. Schiessel: J. Chem. Phys., **119** (2003) 1855.
11) B. Zoetekouwand R. van Roij: Phys. Rev. Lett., **97** (2006) 258302.
12) R. R. Netz: Eur. Phys. J. E, **5** (2001) 557.
13) A. Naji and R. R. Netz: Eur. Phys. J. E, **13** (2004) 43.
14) G. S. Manning: J. Chem. Phys., **51** (1969) 924.
15) R. D. Groot: J. Chem. Phys., **95** (1991) 9191.
16) Y. Levin: Rep. Prog. Phys., **65** (2002) 1577.
17) S. Alexander, P. M. Chaikin, P. Grant, G. J. Morales and P. Pincus: J. Chem. Phys., **80** (1984) 5776.
18) (a) E. Trizac, L. Bocquet and M. Aubouy: Phys. Rev. Lett., **89** (2002) 248301. (b) L. Bocquet, E. Trizac and M. Aubouy: J. Chem. Phys., **117** (2002) 8138.
19) (a) R. W. O'Brien and R. J. Hunter: Can. J. Chem., **59** (1981) 1878. (b) R. W. O'Brien and L. R. White: J. Chem. Soc. Faraday II, **74** (1978) 1607.
20) R. J. Hunter: Zeta Potential in Colloid Science: Principles and Applications, Academic Press, 1981
21) R. J. Hunter: Foundations of Colloid Science, Oxford, 2001
22) W. B. Russel, D. A. Saville and W. R. Schowalter: Colloidal Dispersions, Cambridge, 1989.
23) R. E. Beckham and M. A. Bevan: J. Chem. Phys., **127** (2007) 164708.
24) M. Ishikawa and R. Kitano: Langmuir, **26** (2010) 2438.
25) V. M. Nabutovskii, N. A. Nemov and Y. G. Peisakhovich: Phys. Lett. A, **79** (1980) 98.

(Received 21 Sept. 2010; Accepted 18 May. 2011)